ce/papers Proceedings in civil engineering

Ernst & Sohn A Wiley Brand

ORIGINAL ARTICLE

eurosteel AMSTERDAM 2023

Ernst & Sohn A Wiley Brand

Major-axis buckling of pin-ended stainless steel equal-leg angle section members: FE modelling and design

Behnam Behzadi-Sofiani[1] | M. Ahmer Wadee[1] | Leroy Gardner[1]

Correspondence

Dr. Behnam Behzadi-Sofiani
Department of Civil and Environmental Engineering
Imperial College London
South Kensington Campus
London
United Kingdom
SW7 2AZ
Email: behnam.behzadi-sofiani13@imperial.ac.uk

[1] Imperial College London, London, United Kingdom

Abstract

The behaviour and design of cylindrically-pinned stainless steel equal-leg angle section members under compression and compression combined with strong-axis bending are investigated herein. Numerical models are developed by means of shell finite element modelling formulated within ABAQUS and validated against experimental data. A numerical parametric study is then presented considering both hot-rolled and cold-formed stainless steel equal-leg angle section columns alongside beam-columns with a wide range of cross-section and member geometries. Finally, new design proposals for pin-ended stainless steel equal-leg angle section members under compression and compression plus major-axis bending are developed and verified against the results of physical experiments and numerical simulations. The proposed design rules are shown to offer substantially more accurate and consistent resistance predictions compared to existing codified design rules.

Keywords

Equal-leg angle, Pin-ended angles, Beam-columns, EC3 design procedure

1 Introduction

Angle section members are used in a range of structures, such as towers and trusses alongside the bracing systems in buildings and bridges. Their structural behaviour continues to pose challenges, with current design provisions in international standards known to have significant limitations [1-4]. New resistance functions for angle section members recently developed within the US [1] and European [2, 3] design frameworks have led to substantial improvements in the consistency and accuracy of their load-carrying capacity predictions. The behaviour and design of angles that are cylindrically pinned about the minor axis under combined loading was investigated recently by Behzadi-Sofiani et al. [4]. Angles are often loaded eccentrically such that the point of action does not coincide with the cross-section centroid (see Figure 1). It is therefore crucial to study their behaviour when subjected to compression plus major-axis bending. Behzadi-Sofiani et al. [2, 3] recently developed new design equations for fixed-ended stainless steel angle section columns [2] and beams [3]. These new proposals were then used to establish a new approach for designing pin-ended stainless steel equal-leg angle section members subjected to compression and combined compression and minor-axis bending [4]. The aim of the current paper is to develop new design proposals for cylindrically-pinned stainless steel equal angle section members subjected to compression and combined compression and major-axis bending suitable for incorporation into EN 1993-1-4 [5]. An extensive programme of numerical simulations is presented in Section 3, the observations being summarised in Section 4. Shortcomings in the current design provisions in EC3 are identified using the experimental and numerical results and are highlighted in Section 5. New proposals for the design of stainless steel equal-leg angle section columns and beam-columns cylindrically pinned about the major axis are subsequently presented and assessed against the established data. Statistical analyses are performed that confirm the accuracy of the proposed design method.

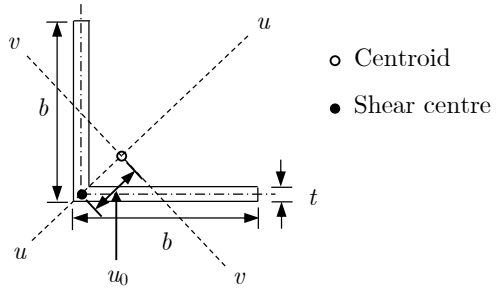

Figure 1 Dimensions and principal axes of equal-leg angles.

2 Review of previous research

Stainless steel equal-leg angle section columns with pin-ended support conditions have been studied in a number of previous investigations [4, 6-14], where they are focused on angle section columns pinned about the minor axis, the findings of which are described in [4]. To the best knowledge of the authors, there has been no experimental investigation reported on stainless steel equal-leg angle section members cylindrically pinned about the major axis, and subjected to compression or combined compression and bending. Therefore, tests were carried out on cylindrically-pinned hot-rolled stainless steel equal-leg angle section members under compression and combined loading, with bending allowed about the major axis. Note that details of the experiments will be reported in a future publication. Numerical models are then validated and are subsequently used to generate additional results to underpin the development of improved design rules for these members.

3 Numerical modelling

The software ABAQUS was used to create numerical models to simulate the mechanical behaviour of stainless steel equal-leg angle section members cylindrically pinned about the major axis and subjected to compression and combined compression and major-axis bending. The FE models are validated in Section 3.2 through comparisons against the new experimental data. In Section 3.3, a parametric study is presented to investigate the behaviour of stainless steel equal-leg angle section columns and beam-columns cylindrically pinned about the major axis.

3.1 General modelling assumptions

Similar modelling assumptions to those used in [2-4] were adopted. The 4-noded shell element, S4R with reduced integration, was employed. A mesh size of approximately 5 mm was utilised. Both hot-rolled and cold-formed stainless steel angles were modelled (further details are provided in [2]). In the validation process, the measured geometric properties and stress-strain curves were employed. Throughout the parametric study, the two-stage Ramberg-Osgood material model [15, 16] was utilised. For the hot-rolled stainless steel angles, a bilinear residual stress distribution with a peak value of 70 MPa was employed [2-4]. For the cold-formed stainless steel angles, the dominant bending residual stresses were assumed to be inherently captured in the material stress-strain curves, and were therefore not explicitly defined. For the validation study, the measured initial minor-axis global bow and twist imperfection amplitudes, were applied; about the major axis, the measured loading eccentricity values, which included the major-axis global bow imperfections, were employed. However, throughout the parametric study, a half-sine wave function over the member length with an amplitude of $L/1000$ at mid-span was adopted about both principal axes for the initial bow imperfections. A similar shape was also adopted for the initial twist with an amplitude of $\vartheta = \tan^{-1}(L/1000b)$ at mid-span.

3.2 Validation

The FE models were validated against the new tests; a summary of the comparisons between the test and FE ultimate resistances is presented in Table 1, where N_u signifies the test/FE ultimate capacity. Overall, there is good agreement between the test and FE ultimate loads.

Table 1 Summary of comparisons of FE model ultimate loads $N_{u,FE}$ with those obtained experimentally $N_{u,Test}$.

No. of tests	$N_{u,FE}/N_{u,Test}$			
	Mean	CoV	Min	Max
7	0.96	0.02	0.94	1.00

3.3 Parametric study

Following validation of the numerical models, a parametric study was conducted. The FE models were used to generate additional data for hot-rolled and cold-formed cylindrically-pinned angle section columns and beam-columns in the three main families of stainless steel (i.e. austenitic, duplex and ferritic), considering a wide range geometries and load combinations. A summary of the material properties adopted in the parametric study is presented in [2]. In total, 2100 FE results were generated. The results are presented in Figure 2, in which the normalised axial load $N_u/N_{b,EC3}$ (where N_u is the test/FE ultimate load and $N_{b,EC3}$ is the member axial compression resistance predicted by EC3) is plotted against the corresponding normalised bending moment $M_u/M_{b,prop}$ (where $M_u = N_u e_0$ is the test/FE ultimate bending moment and $M_{b,EC3}$ is the member bending resistance predicted by EC3). For reference, the interaction curve from prEN 1993-1-4 [17] for I-section members with $\bar{\lambda} = 3.0$ is also shown in the figures.

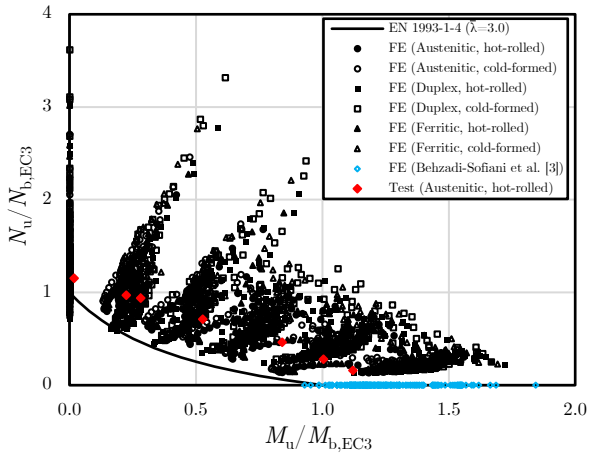

Figure 2 Comparison of test and FE results for stainless steel equal-leg angle section columns and beam-columns cylindrically pinned about the major axis against EC3 interaction curve.

4 Analysis and discussion of results

As can be seen in Figure 2, some of the data points on the vertical axis (i.e. members under axial compression) are on the unsafe side. This is contrary to the observations made in the previous studies [2], where the EC3 predicted buckling loads were conservative for fixed-ended equal-leg angle section columns. It was shown in [4] that when bending about the minor axis is allowed, the buckling resistance of equal-leg angle section columns is reduced due to the shift of the effective centroid. However, this is not the case for angles cylindrically pinned about the major axis, since the shift of the effective centroid only occurs about the minor axis, owing to their symmetry about the major axis. For angle section columns cylindrically pinned

about the major axis, the minor- and major-axis flexural buckling loads are very similar (i.e. $N_{\mathrm{cr,F},u} \approx N_{\mathrm{cr,F},v}$), suggesting that the two global flexural buckling modes could be triggered simultaneously. A study into the elastic post-buckling stability of equal-leg angle section columns, where both ends are fixed about the minor axis, and elastically restrained against rotation about the major axis by a rotational spring, the stiffness k of which varies between zero (i.e. simply supported) and fixed conditions, was conducted. The relationship between normalised load N/N_{cr} and axial shortening δ normalised by the axial shortening at the elastic buckling load δ_{cr} is presented in Figure 3 for an angle section column with slenderness $\bar{\lambda}_{\mathrm{TF}} = 2.5$ but varying rotational stiffness about the major axis. The varying support stiffness about the major axis is also reflected in the $N_{\mathrm{cr,F},u}/N_{\mathrm{cr,F},v}$ ratios, which increase with increasing end-rotation restraint stiffness. The dramatic variation in elastic post-buckling behaviour is clear, where the curves associated with columns with lower $N_{\mathrm{cr,F},u}/N_{\mathrm{cr,F},v}$ ratios (< 2.0) display increasingly negative post-buckling stiffness, which signifies more severe unstable post-buckling.

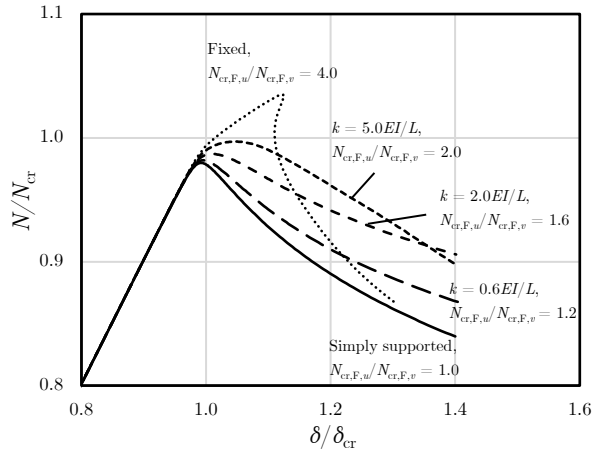

Figure 3 Relationship between normalised load N/N_{cr} and axial shortening δ normalised by the axial shortening at the elastic buckling load δ_{cr} for an angle section column with slenderness $\bar{\lambda}_{\mathrm{TF}} = 2.5$ but varying rotational stiffness about the major axis at the member ends.

To further investigate the influence of the $N_{\mathrm{cr,F},u}/N_{\mathrm{cr,F},v}$ ratio on the buckling resistance of cylindrically-pinned angle section columns, the relationship between the ratio $(\chi_{\mathrm{TF}} - \chi_{\mathrm{F}})/(\chi_{\mathrm{T}} - \chi_{\mathrm{F}})$ in which χ_{TF} is the torsional-flexural reduction factor determined from the FE simulations, χ_{T} is the torsional reduction factor based on the local buckling curve given in EN 1993-1-5 [18] and χ_{F} is the flexural reduction factor based on the flexural buckling curve given in EN 1993-1-1 [5], and the $N_{\mathrm{cr,TF}}/N_{\mathrm{cr,F},v}$ values corresponding to members studied in Figure 3 was plotted in Figure 4. Note that the ratio $(\chi_{\mathrm{TF}} - \chi_{\mathrm{F}})/(\chi_{\mathrm{T}} - \chi_{\mathrm{F}})$ signifies how far the torsional-flexural buckling reduction factor lies between the flexural and local buckling curves. As can be seen, the minimum value of $(\chi_{\mathrm{TF}} - \chi_{\mathrm{F}})/(\chi_{\mathrm{T}} - \chi_{\mathrm{F}})$ reduces with decreasing rotational spring stiffness. This means that the level of interaction between torsional-major-axis-flexural and minor-axis-flexural buckling is even more significant when the rotational restraint about the major axis is reduced. This relationship may also be shown through the $N_{\mathrm{cr,F},u}/N_{\mathrm{cr,F},v}$ ratio, where the newly proposed term β (as described in Section 6.1), which accounts for the reduction in buckling resistance due to the aforementioned interaction, varies with $N_{\mathrm{cr,F},u}/N_{\mathrm{cr,F},v}$, with a maximum magnitude at $N_{\mathrm{cr,F},u}/N_{\mathrm{cr,F},v} = 1.0$ and a minimum value at $N_{\mathrm{cr,F},u}/N_{\mathrm{cr,F},v} =$ 4.0. The aforementioned observations dictate the necessity for a new definition for β compared to that proposed in [2] to capture the influence of different boundary conditions on the severity of interaction interactive buckling.

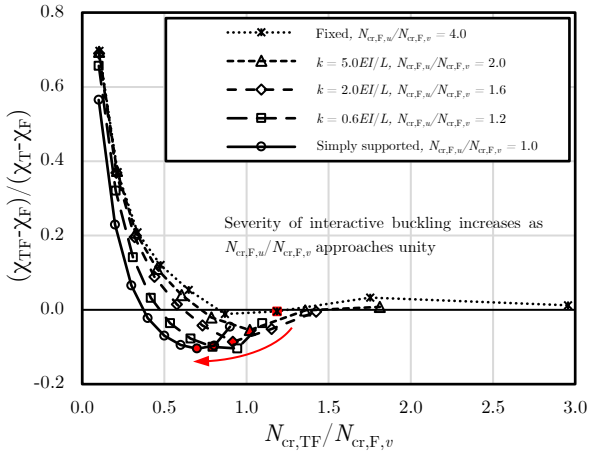

Figure 4 Variation of $(\chi_{\mathrm{TF}} - \chi_{\mathrm{F}})/(\chi_{\mathrm{T}} - \chi_{\mathrm{F}})$ with $N_{\mathrm{cr,TF}}/N_{\mathrm{cr,F},v}$ for angle section columns with $\bar{\lambda}_{\mathrm{TF}} = 2.5$, where both ends are fixed about the minor axis and elastically restrained about the major axis.

5 Design to Eurocode 3

For angles under compression, the buckling resistance $N_{\mathrm{b,Rd}}$ is given by:

$$N_{\mathrm{b,Rd}} = \frac{\chi A f_{\mathrm{y}}}{\gamma_{\mathrm{M1}}}, \tag{1}$$

where A is the cross-sectional area, replaced by the effective area A_{eff} for Class 4 cross-sections [18], χ is the buckling reduction factor and γ_{M1} is the member buckling partial factor, taken as $\gamma_{\mathrm{M1}} = 1.0$ for stainless steel. According to prEN 1993-1-4 [17], angles subjected to combined loading with bending about the major u-u axis and axial compression should satisfy the following criterion:

$$\frac{N_{\mathrm{Ed}}}{\frac{\chi_u N_{\mathrm{Rk}}}{\gamma_{\mathrm{M1}}}} + k_{uu}\frac{M_{u,\mathrm{Ed}} + \Delta M_{u,\mathrm{Ed}}}{\frac{M_{u,\mathrm{Rk}}}{\gamma_{\mathrm{M1}}}} \leq 1.0 \tag{2}$$

Here, N_{Ed} and $M_{u,\mathrm{Ed}}$ are the design values of the compression force and maximum bending moment about the major u-u axis, respectively, and N_{Rk} and $M_{u,\mathrm{Rk}}$ are the characteristic cross-sectional resistance to compressive axial force and bending moment about the major u-u axis, respectively. The quantity $\Delta M_{u,\mathrm{Ed}}$ is the bending moment due to the shift of the effective centroid about the major u-u axis, eN_{u}, for Class 4 cross-sections, which is zero for equal-leg angle section members, owing to their symmetry about the major axis. The term χ_u is the flexural buckling reduction factor, which should be replaced by χ_{TF} for members where torsional-flexural buckling is critical, while k_{uu} is the interaction factor defined thus:

$$k_{uu} = \begin{cases} 1 + 2.5(\bar{\lambda} - 0.35)n_u & \text{for } \bar{\lambda} < 1.0 \\ 1 + 1.625n_u & \text{for } \bar{\lambda} \geq 1.0 \end{cases} \tag{3}$$

in which $\bar{\lambda}$ is replaced by $\bar{\lambda}_{\mathrm{TF}}$ when torsional-flexural buckling is critical and n_u is given as follows:

$$n_u = \frac{N_{\mathrm{Ed}}}{\chi_u N_{\mathrm{Rk}}/\gamma_{\mathrm{M1}}} \tag{4}$$

noting Equation (4) is specified in prEN 1993-1-4 [17] for I-section members and is assumed to be also applicable to angles. Comparisons of the test and FE ultimate capacities

with the EC3 resistances are made in Figure 5, where R_u and $R_{b,Rd}$ are the test/FE ultimate capacity and the resistance under combined loading, with $R_{b,EC3}$ and $R_{b,prop}$ referring to the EC3 [17] and proposed resistances. The angle θ is illustrated in Figure 6.

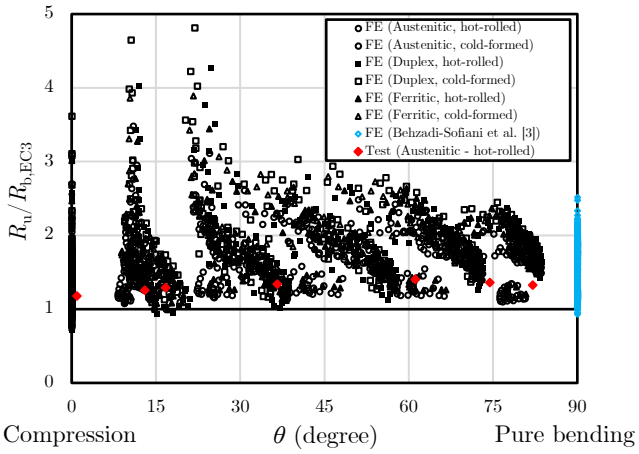

Figure 5 Comparisons of test and FE results with EC3 ultimate capacities for stainless steel equal-leg angle section columns and beam-columns cylindrically pinned about the major axis.

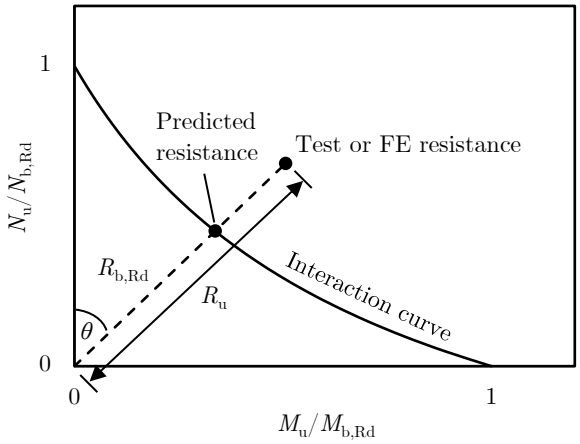

Figure 6 Definition of parameters R_u, $R_{b,Rd}$, θ.

The EC3 resistance predictions can be seen to be scattered. The conservative predicted resistances for low θ values, where compression is dominant, is due to the double-counting of the same buckling mode (i.e. torsional and local buckling) [1, 2]. In addition, the lack of consideration of interactive buckling, described in Section 4, leads to unsafe results. On the other hand, the EC3 treatment for the simultaneous occurrence of both local and lateral-torsional buckling for major-axis bending has shown to be conservative [3], and becomes dominant for high θ values. A new interaction curve, anchored to the end points determined based on the new proposals in Section 6, is needed to provide more accurate resistance predictions for stainless steel equal-leg angle section columns and beam-columns cylindrically-pinned about the major-axis.

6 New design proposals

Recent proposals for the design of stainless steel equal-leg angle section fixed-ended columns [2] and beams [3], along with the findings presented in Section 4, are adopted in the current paper to develop new proposals for the design of cylindrically-pinned stainless steel angle section columns and beam-columns with bending about the major axis. The proposed new design formula is given by:

$$\frac{N_{Ed}}{N_{b,Rd}} + k_{uu}\frac{M_{u,Ed} + \Delta M_{u,Ed}}{M_{b,u,Rd}} \leq 1.0 \quad (5)$$

where $N_{b,Rd}$ and $M_{b,u,Rd}$ are the member buckling resistances under axial compression and bending about the major u-u axis, respectively. The new proposals for $N_{b,Rd}$ [2] and $M_{b,u,Rd}$ [3], with some modifications to reflect the findings reported in Section 4, are summarised below.

6.1 Member buckling resistance under axial compression

6.1.1 *Torsional-flexural buckling critical (i.e. $N_{cr,TF} \leq N_{cr,F,v}$)*

The proposed design expression for determining the buckling resistance of stainless steel equal-leg angle section members under compression [2] when torsional-flexural buckling is critical, is given thus:

$$N_{b,Rd} = \frac{\chi_{TF} A f_y}{\gamma_{M1}} \quad (6)$$

noting that the gross area A is used for all classes of cross-section. In Equation (6):

$$\chi_{TF} = \chi_F + \Delta_F(\chi_T - \chi_F) \quad (7)$$

the torsional χ_T and flexural χ_F buckling reduction factor are given by:

$$\chi_T = \frac{\bar{\lambda}_{TF} - 0.188}{\bar{\lambda}_{TF}^2} \text{ but } \chi_T \leq 1.0 \quad (8)$$

$$\chi_F = \frac{1}{\phi + \sqrt{\phi^2 - \bar{\lambda}_{TF}^2}} \text{ but } \chi_F \leq 1.0 \quad (9)$$

and Δ_F is given thus:

$$\Delta_F = \left(1 - \frac{N_{cr,TF}}{N_{cr,F,v}}\right)^p \quad (10)$$

Where

$$p = \begin{cases} 2.0\bar{\lambda}_{TF} & \text{for } \bar{\lambda}_{TF} < 2.0 \\ 2.93\bar{\lambda}_{TF}^{0.45} & \text{for } \bar{\lambda} \geq 2.0 \end{cases} \quad (11)$$

with the torsional-flexural slenderness $\bar{\lambda}_{TF}$ and ϕ being given thus:

$$\bar{\lambda}_{TF} = \sqrt{\frac{A f_y}{N_{cr,TF}}} \quad (12)$$

$$\phi = 0.5[1 + \alpha\beta_{max}(\bar{\lambda}_{TF} - 0.2)^{\beta_{max}} + \bar{\lambda}_{TF}^2] \quad (13)$$

Where

$$\beta_{max} = 1.77 - 0.08\left(\frac{N_{cr,F,u}}{N_{cr,F,v}}\right) \text{ but } \beta_{max} \geq 1.45 \quad (14)$$

For the imperfection factor α, values of 0.6 and 0.49 are recommended for hot-rolled and cold-formed stainless steel angles, respectively.

6.1.2 *Minor-axis flexural buckling critical (i.e. $N_{cr,F,v} < N_{cr,TF}$)*

The proposed design expression for determining the buckling resistance of stainless steel equal-leg angle section members under axial compression [2], when minor-axis flexural buckling is critical is:

$$N_{b,Rd} = \frac{\chi_F A f_y}{\gamma_{M1}} \quad (15)$$

Where

$$\chi_F = \frac{1}{\phi + \sqrt{\phi^2 - \bar{\lambda}^2}} \quad \text{but} \quad \chi_F \leq 1.0 \tag{16}$$

in which the normalised slenderness $\bar{\lambda}$ and ϕ are given by:

$$\bar{\lambda} = \sqrt{\frac{Af_y}{N_{cr,F,v}}} \tag{17}$$

$$\phi = 0.5[1 + \alpha\beta(\bar{\lambda} - 0.2)^{\beta} + \bar{\lambda}^2] \tag{18}$$

with β being a factor allowing for the influence of interactive buckling given by:

$$\beta = \beta_{max} + (1 - \beta_{max})\left(\frac{N_{cr,TF}}{N_{cr,F,v}}\right) \quad \text{but} \quad 1.0 \leq \beta \leq \beta_{max} \tag{19}$$

The imperfection factor remains as specified above: $\alpha = 0.6$ and $\alpha = 0.49$ for hot-rolled and cold-formed stainless steel angles, respectively.

6.2 Member buckling resistance under major-axis bending

For determining the member buckling resistance of stainless steel equal-leg angle section members under major-axis bending, the following expression is proposed [3]:

$$M_{b,u,Rd} = \frac{\chi W_{pl,u} f_y}{\gamma_{M1}} \tag{20}$$

in which the plastic section modulus $W_{pl,u}$ is used for all classes of cross-section. In Equation (20):

$$\chi = \chi_{LT} + \Delta(\chi_l - \chi_{LT}) \tag{21}$$

in which the local χ_l and lateral-torsional χ_{LT} buckling reduction factor are given by:

$$\chi_l = \frac{\bar{\lambda}_{max,u} - 0.188}{\bar{\lambda}^2_{max,u}} \quad \text{but} \quad \chi_l \leq 1.0 \tag{22}$$

$$\chi_{LT} = \frac{1}{\phi_{LT} + \sqrt{\phi^2_{LT} - \bar{\lambda}^2_{max,u}}} \quad \text{but} \quad \chi_{LT} \leq 1.0 \tag{23}$$

and Δ is given thus:

$$\Delta = \begin{cases} \left(1 - \frac{M_{cr,l,u}}{M_{cr,LT,u}}\right)^{3.5} & \text{for} \quad \frac{M_{cr,l,u}}{M_{cr,LT,u}} \leq 1.0 \\ 0 \quad \text{for} \quad \frac{M_{cr,l,u}}{M_{cr,LT,u}} > 1.0 \end{cases} \tag{24}$$

with the maximum normalised slenderness $\bar{\lambda}_{max,u}$ and ϕ_{LT} being given thus:

$$\bar{\lambda}_{max,u} = \sqrt{\frac{W_{pl,u} f_y}{M_{cr}}} \tag{25}$$

$$\phi_{LT} = 0.5[1 + \alpha_{LT}(\bar{\lambda}_{max,u} - \bar{\lambda}_{LT,0}) + \bar{\lambda}^2_{max,u}] \tag{26}$$

where M_{cr} is the minimum of the local $M_{cr,l,u}$ and the major-axis lateral-torsional $M_{cr,LT,u}$ critical buckling moments. The proposed values for the imperfection factor α_{LT} and limiting slenderness $\bar{\lambda}_{LT,u}$, are 0.49 and 0.4, respectively, for both hot-rolled and cold-formed stainless steel angles.

6.3 Interaction factor k_{uu}

The suitability of the existing interaction factor k_{uu} for use with the new proposed axial and bending resistances is assessed herein. The expression for the interaction factor k_{uu} takes the general bilinear form given thus:

$$k_{uu} = 1 + (D_1\bar{\lambda} + D_2)n_u \tag{27}$$

where D_1 and D_2 are constants. Equation (27) can be rearranged into the following expression:

$$\frac{k_{uu} - 1}{n_u} = D_1\bar{\lambda} + D_2 \tag{28}$$

The test and FE $(k_{uu} - 1)/n_u$ values are plotted against the critical normalised slenderness, $\bar{\lambda}_{TF}$ or $\bar{\lambda}$, in Figure 7. The bilinear EC3 expression for the interaction factor for I-sections is also shown, and can be seen to lie generally on the safe side of (i.e. above) the experimental and numerical results, but excessively so. New expressions were therefore sought that provide a closer match to the data; the following expressions are proposed:

$$k_{uu} = \begin{cases} 1 + (3\bar{\lambda} - 1)n_u & \text{for } \bar{\lambda} \leq 0.5 \\ 1 + 0.5n_u & \text{for } \bar{\lambda} > 5.0 \end{cases} \tag{29}$$

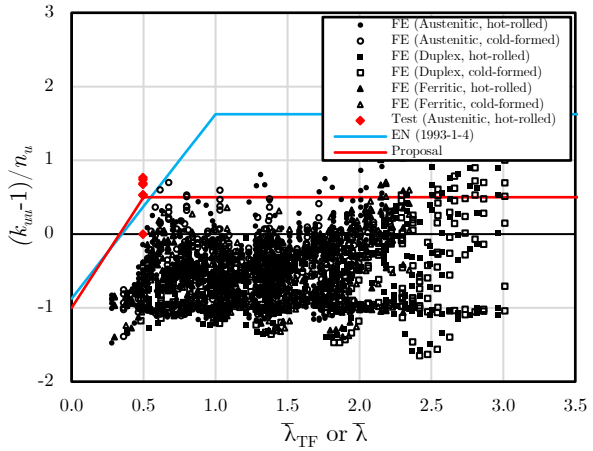

Figure 7 Comparisons of test and FE results with the existing EC3 and proposed interaction factors k_{uu} for combined compression and bending about the major axis.

6.4 Assessment of design proposals

A summary of the comparisons of the test and FE capacities R_u with the newly proposed resistance predictions $R_{b,prop}$ is presented in Figure 8.

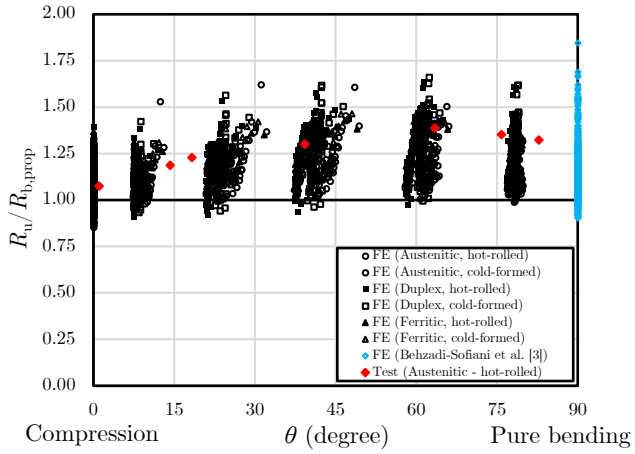

Figure 8 Comparisons of test and FE results with resistance predictions according to the new proposals for stainless steel equal-leg angle section columns and beam-columns cylindrically pinned about the major axis.

By comparing Figure 5 and Figure 8, it can be seen that the resistance predictions are significantly improved for pin-ended stainless steel angles under compression and combined loading using the new proposals relative to the current Eurocode 3 provisions.

7 Conclusions

A comprehensive study into the behaviour and design of pin-ended stainless steel equal-leg angle section members subjected to compression and combined compression and major-axis bending has been presented herein. Finite element models were developed and validated against the test results. A parametric study was subsequently conducted on both hot-rolled and cold-formed angle section columns and beam-columns in austenitic, duplex and ferritic stainless steel covering a spectrum of cross-section and member geometries and load combinations. The test and FE results were used to assess the current EC3 design provisions for pin-ended stainless steel equal-leg angle section columns and beam-columns bending about the major axis. The resistance predictions were found to be highly scattered relative to the test and numerical data, with predictions both on the unsafe and conservative side. For column buckling resistance, the current EC3 design provisions account for torsional/local buckling twice, which is the primary source of the observed conservatism. However, for slender columns the lack of account for interactive buckling, the severity of which was shown to vary for different boundary conditions, leads to unsafe predictions. New expressions were proposed to reflect the variation of the severity of interactive buckling for different boundary conditions through the $N_{\mathrm{cr,F},u}/N_{\mathrm{cr,F},v}$ ratio. For angles subjected to major-axis bending, the simultaneous consideration of local and lateral-torsional buckling, while only one buckling mode is critical, results in conservative predictions. These issues, together with an absence of a specific interaction curve for angle section members, lead to the inaccurate EC3 resistance predictions. A new design approach for cylindrically-pinned stainless steel angle section members under compression and combined loading, reflecting the above findings has been proposed. Overall, the new design proposals have been shown to lead to significantly more accurate resistance predictions for both hot-rolled and cold-formed cylindrically-pinned stainless steel equal-leg angle section columns and beam-columns.

References

[1] Dinis, P. B.; Camotim, D. (2015) *A novel DSM-based approach for the rational design of fixed-ended and pin-ended short-to-intermediate thin-walled angle columns*, Thin-Walled Struct. 87 158–182.

[2] Behzadi-Sofiani, B.; Gardner, L.; Wadee, M. A. (2021) *Stability and design of fixed-ended stainless steel equal-leg angle section columns*, Eng. Struct. 249 113281.

[3] Behzadi-Sofiani, B.; Gardner, L.; Wadee, M. A. (2022) *Testing, numerical analysis and design of stainless steel equal-leg angle section beams*, Structures 37 977–1001.

[4] Behzadi-Sofiani, B.; Wadee, M. A.; Gardner, L. (2023) *Testing, FE modelling and design of pin-ended stainless steel equal-leg angle section columns and beam-columns*, J. Constr. Steel Res. 208 107973.

[5] EN 1993-1-4 (2006) *Eurocode 3: Design of steel structures – Part 1-4: General rules – Supplementary rules for stainless steels*, European Committee for Standardisation (CEN), Brussels.

[6] Filipovic, A.; Dobric, J.; Baddoo, N.; Moze, P. (2021) *Experimental response of hot-rolled stainless steel angle columns*, Thin-Walled Struct. 163 107659.

[7] Filipovic, A.; Dobric, J.; Budevac, D.; Fric, N.; Baddoo, N. (2021) *Experimental study of laser-welded stainless steel angle columns*, Thin-Walled Struct. 164 107777.

[8] Dobric, J.; Filipovic, A.; Markovic, Z.; N. Baddoo (2020) *Structural response to axial testing of cold-formed stainless steel angle columns*, Thin-Walled Struct. 156 106986.

[9] Reynolds, N. A. (2013) *Behavior and design of concentrically loaded duplex stainless steel single equal-leg angle struts*, Ph.D. thesis, Georgia Institute of Technology.

[10] Zhang, L.; Liang, Y.; Zhao, O. (2020) *Experimental and numerical investigations of pin-ended hot-rolled stainless steel angle section columns failing by flexural buckling*, Thin-Walled Struct. 156 106977.

[11] Zhang, L.; Liang, Y.; Zhao, O. (2021) *Laboratory testing and numerical modelling of pin-ended hot-rolled stainless steel angle section columns failing by flexural-torsional buckling*, Thin-Walled Struct. 161 107395.

[12] Dobric, J.; Filipovic, A.; Baddoo, N.; Markovic, Z.; Budevac, D. (2021), *Design procedures for cold-formed stainless steel equal-leg angle columns*, Thin-Walled Struct. 159 107210.

[13] Dobric, J.; Filipovic, A.; Baddoo, N.; Budevac, D.; Rossi, B. (2021) *Design criteria for pin-ended hot-rolled and laser-welded stainless steel equal-leg angle columns*, Thin-Walled Struct. 167 108175.

[14] Dobric, J.; Filipovic, A.; Baddoo, N.; Markovic Z.; Budevac, D. (2021) *The new buckling curves for cold-formed stainless steel equal-leg angle columns*, in: ASES International congress proceedings/Association of Structural Engineers of Serbia, 16th Congress, pp. 501–510.

[15] Gardner, L.; Yun, X. (2018) *Description of stress–strain curves for cold-formed steels*, Construction and Building Materials 189 527–538.

[16] Yun, X.; Wang, Z.; Gardner, L. (2021) *Full-range stress–strain curves for aluminium alloys*, J. Struct. Eng. 147 (6) 04021060.

[17] prEN 1993-1-4 (2020) *Eurocode 3: Design of steel structures – Part 1-4: General rules – Supplementary rules for stainless steels*, European Committee for Standardisation (CEN), Brussels, final document.

[18] EN 1993-1-5 (2006) *Eurocode 3: Design of steel structures – Part 1-5: Plated structural elements,* European Committee for Standardisation (CEN), Brussels.